

RESEARCH

Open Access



# Exploring the predictive value of carotid Doppler ultrasound and clinical features for spinal anesthesia-induced hypotension: a prospective observational study

Esmée C. de Boer<sup>1,2\*</sup>, Joris van Houte<sup>2</sup>, Catarina Dinis Fernandes<sup>1</sup>, Tom Bakkes<sup>1</sup>, Jens Muehlsteff<sup>3</sup>, R. Arthur Bouwman<sup>1,2</sup> and Massimo Mischi<sup>1</sup>

## Abstract

**Background** The induction of spinal anesthesia is often followed by hypotension, which has been associated with post-operative end-organ damage. A timely prediction of spinal anesthesia-induced hypotension (SAIH) paired with appropriate interventions may reduce the risk of adverse outcomes. This study investigated the value of carotid Doppler ultrasound measurements and clinical variables, both individually and combined, to predict SAIH.

**Methods** Adult patients who were scheduled for elective surgery under spinal anesthesia were included. Carotid ultrasound imaging and baseline vital sign measurements were performed pre-operatively, well in advance of the induction of spinal anesthesia. The occurrence of hypotension was observed for ten minutes after the induction of spinal anesthesia. Logistic regression models studied linear relationships within the derived set of ultrasound and clinical features, and support vector machine models evaluated nonlinear relationships.

**Results** A total of 40 patients were included, and 45% of them developed SAIH. The logistic regression models performed better than the support vector machine models. The best-performing logistic regression model combined carotid ultrasound and clinical features and had a sensitivity of 75 [73–81]%, specificity of 75 [71–81]%, AUROC of 0.81 [0.75–0.95], positive predictive value of 75 [65–81]%, negative predictive value of 75 [71–88]% and F1 score of 0.75 [0.71–0.76]. The key features that were shown to predict SAIH were baseline mean arterial pressure, fasting time, ASA class, and weight.

**Conclusions** Combining carotid Doppler ultrasound measurements and clinical variables can predict the occurrence of SAIH.

**Trial registration** The study was retrospectively registered at clinicaltrials.gov (NCT06711289) on 2 December 2024.

**Keywords** Spinal anesthesia-induced hypotension, Carotid Doppler ultrasound, Machine learning, Hypotension prediction

\*Correspondence:

Esmée C. de Boer  
e.c.d.boer@tue.nl

Full list of author information is available at the end of the article



© The Author(s) 2025. **Open Access** This article is licensed under a Creative Commons Attribution-NonCommercial-NoDerivatives 4.0 International License, which permits any non-commercial use, sharing, distribution and reproduction in any medium or format, as long as you give appropriate credit to the original author(s) and the source, provide a link to the Creative Commons licence, and indicate if you modified the licensed material. You do not have permission under this licence to share adapted material derived from this article or parts of it. The images or other third party material in this article are included in the article's Creative Commons licence, unless indicated otherwise in a credit line to the material. If material is not included in the article's Creative Commons licence and your intended use is not permitted by statutory regulation or exceeds the permitted use, you will need to obtain permission directly from the copyright holder. To view a copy of this licence, visit <http://creativecommons.org/licenses/by-nc-nd/4.0/>.

## Introduction

Hypotension is a common side effect of anesthesia, with reported incidences varying from 19 to 70% (Bijker et al. 2007; Chowdhury et al. 2023; Sessler et al. 2019). The depth and duration of intraoperative hypotension are associated with the occurrence and extent of post-operative end-organ failure (e.g., acute kidney injury and myocardial damage) and death, although a direct causal relationship has not been established (Sessler et al. 2019; Walsch et al. 2013; Wesselink et al. 2018). Spinal anesthesia involves the administration of an intrathecal local anesthetic that blocks the sympathetic nervous system. This leads to reduced systemic vascular resistance and left ventricular preload, resulting in spinal anesthesia-induced hypotension (SAIH) in up to half of the patients (Chowdhury et al. 2023; Jakobsson et al. 2017; Kim et al. 2022; Meyhoff et al. 2009).

The depth and duration of the hypotensive period may be reduced with prophylactic administration of fluids or vaso-active medication (Mendonça et al. 2021). However, excessive co-loading with crystalloids may result in fluid overload, which is associated with complications such as pulmonary edema, renal dysfunction, and poor surgical outcomes (Mendonça et al. 2021; Rivers et al. 2001). This emphasizes the necessity of predicting SAIH before performing spinal anesthesia, which enhances the anesthesiologist's vigilance and promotes a proactive instead of a reactive approach.

Lin et al. (Lin et al. 2008) built an artificial neural network using clinical, surgical, and anesthetic variables to predict hypotensive periods during spinal anesthesia and reached a model performance with a sensitivity of 76%, specificity of 76%, and area under the receiver characteristic curve (AUROC) of 0.80. Since one of the features was extracted during the spinal anesthesia procedure—the local anesthetic dose—this model will result in little gain for timely reactions for anesthesiologists.

Previous studies identified several clinical variables as risk factors for SAIH such as age (Singla et al. 2006; Tarkkila and Isola 1992), baseline blood pressure (Carpenter et al. 1992; Singla et al. 2006), body mass index (BMI) (Hartmann et al. 2002; Singla et al. 2006; Tarkkila and Isola 1992), and peak block height (Carpenter et al. 1992; Singla et al. 2006; Tarkkila and Isola 1992). The risk of SAIH is further increased by pre-operative hypovolemia, which may occur due to preoperative fasting, bowel preparation, or chronic illness.

Over the last decade, the corrected carotid flow time (ccFT), a parameter obtained from carotid Doppler ultrasound (CDU), was shown to be associated with fluid responsiveness (Barjaktarevic et al. 2018; Suriyani et al. 2022). More recently, the ccFT has also been

demonstrated to be a promising predictor of hypotension after the induction of general anesthesia (Maitra et al. 2020; Wang et al. 2022), and a predictor of SAIH in parturient women (Kim et al. 2021). However, its potential to predict SAIH in non-cardiac surgery patients could not yet be confirmed (van Houte et al. 2024; Kim et al. 2022). The development of carotid ultrasound patches allows noninvasive and continuous measurement of central blood flow characteristics (Kenny et al. 2021; Wang et al. 2022). As such, additional and potentially relevant carotid ultrasound features that may predict SAIH can be extracted. While current research has primarily focused on known and well-established CDU-derived parameters, such as the ccFT, the full potential of this technology remains underexplored.

This study aimed to investigate the use of simple landmarks and new features derived from CDU to predict SAIH, alongside clinical parameters. Both linear and nonlinear models were evaluated and we further explored whether CDU could enhance SAIH timely prediction. This information is valuable in identifying patients at increased risk of SAIH, providing anesthesiologists with ample time to intervene.

## Methods

### Study design

Previously acquired data (van Houte et al. 2024) were used to perform the analysis. This prospective observational study was performed in the Catharina Hospital in Eindhoven, The Netherlands, from April to September 2023 and was approved by the Medical Research Ethics Committees United (W22.234).

### Subjects

Adult patients who were scheduled for elective orthopedic, gynecologic, or urologic surgery under spinal anesthesia were screened preoperatively for their eligibility for study participation. Patients with conditions or factors that could affect carotid blood flow were excluded from study participation to ensure the accuracy and reliability of study results. Specifically, patients were excluded if they had contra-indications for spinal anesthesia, emergency surgery, poor left or right ventricular function (ejection fraction  $\leq 40\%$ ), moderate to severe valvular disease, atrial fibrillation, pacemaker rhythm, carotid artery stenosis  $> 50\%$ , history of cerebrovascular accident or transient ischemic attack, history of cerebral trauma, pregnancy, neck complaints, and morbid obesity (BMI  $\geq 40$  kg/m<sup>2</sup>). Images were excluded from the analysis if the ultrasound image quality was insufficient. Eligible patients were included upon receiving informed consent.

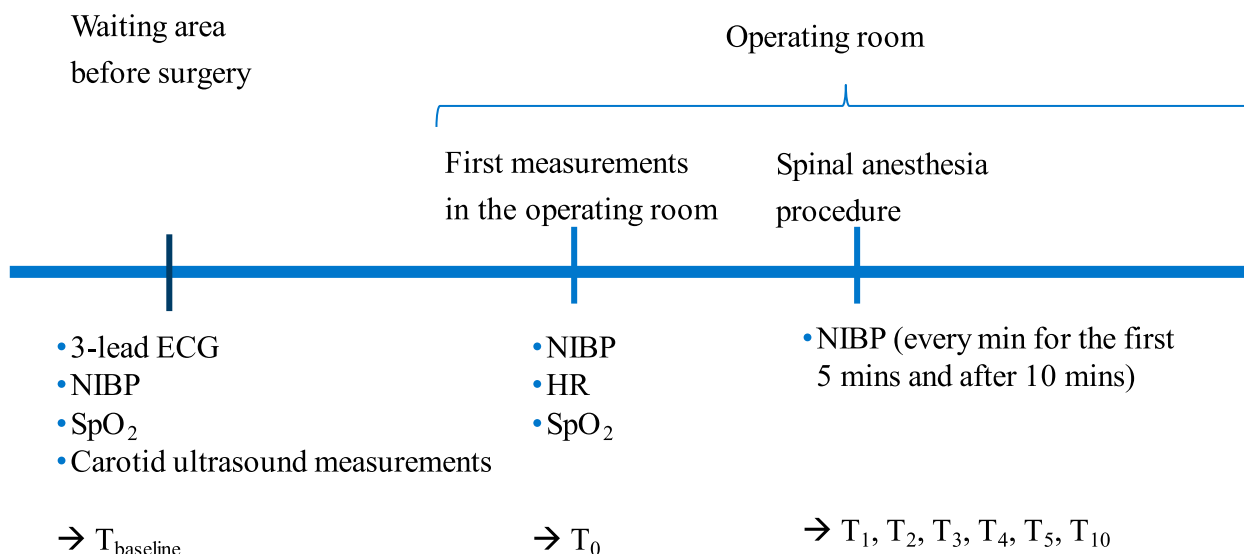


**Fig. 1** Timeline of the study protocol. ECG: electrocardiogram, HR: heart rate, NIBP: noninvasive blood pressure, SpO<sub>2</sub>: peripheral oxygen saturation

### Ultrasound imaging

Ultrasound acquisitions were performed using a commercially available Affiniti 70 machine equipped with a linear array probe of 4–15 MHz (L15-4 broadband linear array transducer, Philips Healthcare, Best, The Netherlands). Images were acquired using duplex mode, i.e., simultaneous B-mode and pulsed-wave Doppler (PWD).

### Study protocol

Figure 1 illustrates a timeline of the data acquisition process. While they awaited their surgery, patients were placed in the supine position without a pillow, with the head of the bed elevated at 15°. They were asked to slightly rotate their heads to the contralateral side and breathe comfortably without taking deep breaths. Pre-anesthetic monitoring consisted of three-lead electrocardiography (ECG), noninvasive blood pressure monitoring (NIBP), and pulse oximetry recorded directly before the CDU acquisitions started. The average value of two blood pressure measurements, obtained directly before CDU acquisitions of the left and right carotid arteries, was considered as the patient's baseline blood pressure value ( $T_{\text{baseline}}$ ).

Ultrasound measurements were performed on the right and left common carotid artery. First, the artery was visualized in the short-axis and long-axis views to scan for stenoses and extensive atherosclerotic lesions. Subsequently, the PWD mode was activated using a sample volume size of 2.5 mm, an insonation angle of 60°, and the medium speed setting (33 mm/s). An acquisition was obtained in the long-axis view, 2 cm below the

carotid bifurcation. The acquisition was saved as a still image lasting 6.6 s and captured 6 to 8 beats depending on the patient's heart rate, see Fig. 2. Carotid ultrasound imaging was performed by an experienced sonographer (> 10 years of experience).

Next, the patient was transferred to the operating room. Right before the induction of spinal anesthesia, the blood pressure was measured ( $T_0$ ). The attending anesthesiologist responsible for the patient performed the spinal anesthesia procedure and determined the type of the local anesthetic. The dosage was determined based on the patient's height. The blood pressure was measured once every minute for the first five minutes ( $T_1$  to  $T_5$ ) and ten minutes ( $T_{10}$ ) after the induction of spinal anesthesia. During these ten minutes, the patient's position remained unaltered (no-touch period). The lowest systolic blood pressure (SBP) and mean arterial pressure (MAP) values were recorded and used to calculate the magnitude of SBP and MAP decrease compared to  $T_{\text{baseline}}$ . In the case of hypotension, the attending anesthesiologist treated the patient per clinical protocol by administering fluids or vasoactive medication (e.g., phenylephrine or ephedrine). Hypotension was defined as either:

- SBP reduction of >30% or MAP reduction of >20% from baseline, or
- an absolute SBP <90 mmHg or an absolute MAP <65 mmHg, or
- the onset of hypotension-related symptoms, e.g., dizziness, nausea, or vomiting.

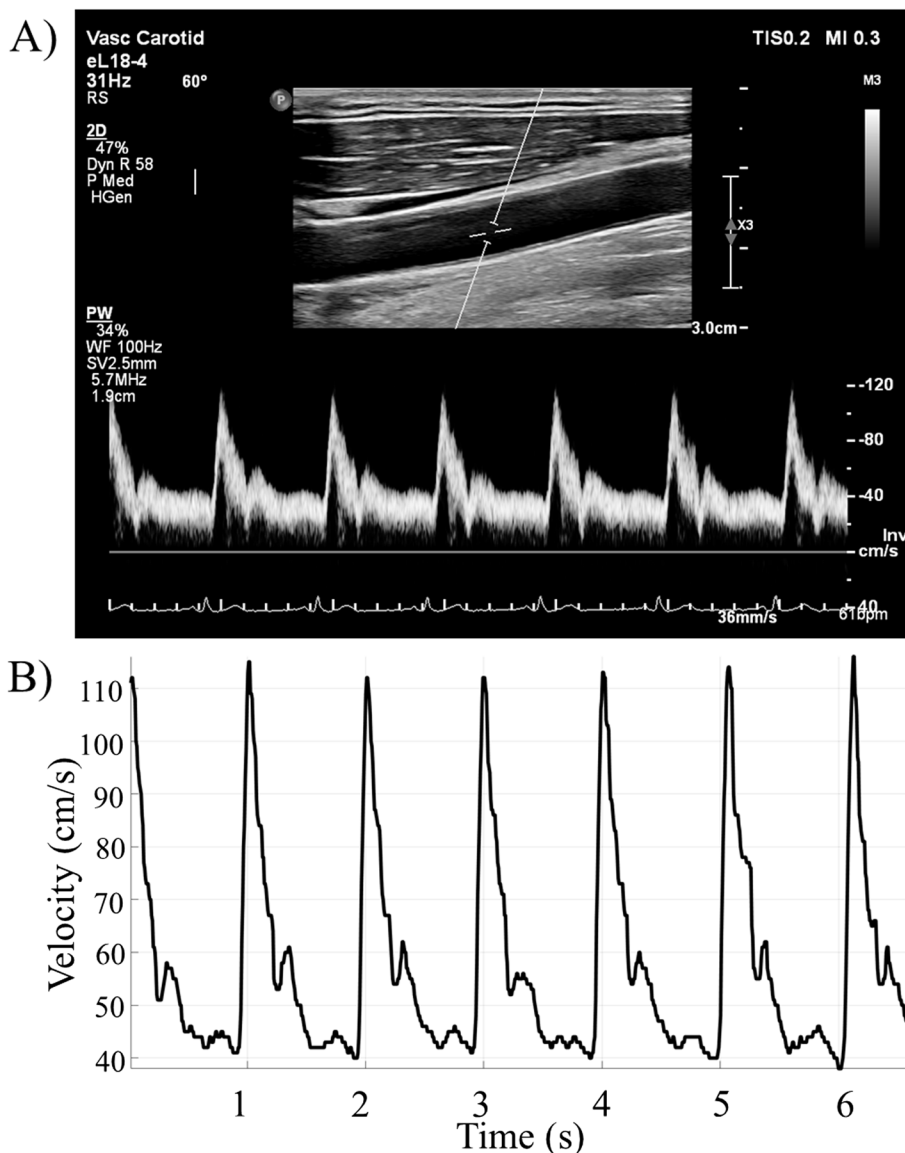


**Fig. 2** Analysis of the velocity waveform. **A** Original ultrasound image. **B** Extracted velocity waveform

**Analysis**

Data analysis was performed in Matlab R2023a (Mathworks, MA, USA). Relevant features were obtained from the electronic health record, baseline blood pressure measurements, and carotid ultrasound images and used to build logistic regression and support vector machine (SVM) models.

**Analysis of the carotid ultrasound images**

The velocity waveform was extracted from the carotid ultrasound image by computing the maximal envelope of the PWD waveform, see Fig. 2A and B. From this waveform, an ensemble average was computed. Features

were extracted from the full waveform and the ensemble average waveform. See Appendix A1 for a detailed description of this analysis. All waveforms were visually cross-checked for artifacts or erroneous landmark detection. In such a case, the landmarks were manually revised. The values obtained from the left and right carotid arteries were averaged, such that one value was obtained per patient.

**Feature extraction**

In total, 28 features were studied, of which 20 were derived from the carotid velocity waveform. Fig. 3

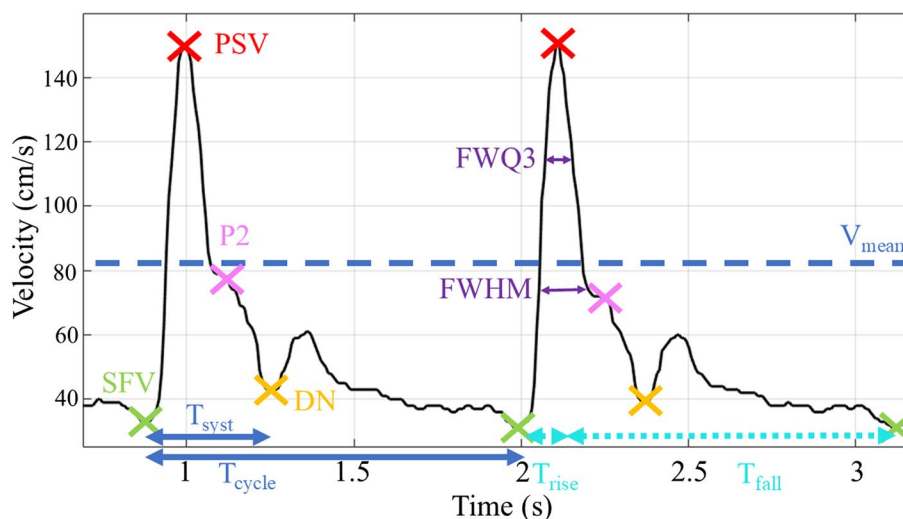


**Fig. 3** Carotid ultrasound velocity waveform with landmarks used to compute the features. The peak systolic velocities (PSV) are indicated with red crosses. The systolic foot velocities (SFV) are marked with green crosses and divide the waveform into individual beats. The secondary systolic peaks (P2) are indicated with pink crosses. Yellow crosses indicate the dicrotic notch (DN). The dashed line indicates the mean velocity value over the entire velocity waveform ( $V_{\text{mean}}$ ). The systolic flow time ( $T_{\text{syst}}$ ), indicated by the thick, short, blue arrow, is the time from the SFV until the DN. The cycle time ( $T_{\text{cycle}}$ ) is the duration of one heartbeat, indicated by the thick, long, blue arrow. The thin, purple arrows within the right beat indicate the full-width half-maximum (FWHM, bottom arrow) and full-width at 75% of the maximal amplitude (FWQ3, upper arrow). The dotted, light-blue arrows indicate the rise time ( $T_{\text{rise}}$ , short arrow, from SFV to PSV) and fall time ( $T_{\text{fall}}$ , long arrow, from PSV to SFV). DN: dicrotic notch, FWHM: full-width half-maximum, FWQ3: full-width at 75% of the maximal amplitude, P2: secondary systolic peak, PSV: peak systolic velocity, SFV: systolic foot velocity,  $T_{\text{cycle}}$ : cycle time,  $T_{\text{fall}}$ : fall time,  $T_{\text{syst}}$ : systolic flow time,  $T_{\text{rise}}$ : rise time

displays landmarks that were determined to compute the CDU-based features. Eight features were obtained from the electronic health record and vital sign baseline measurements. Table 1 contains an overview of all features investigated in this study.

#### Logistic regression model

With the intent of feature dimensionality reduction, cross-correlation with transitive closure was used to remove highly correlated features (Pearson correlation coefficient  $>0.8$ ). Transitive closure identified groups of highly correlated feature pairs (Henzinger and King 1995). Per group of correlated features, the feature with the highest correlation with the label was selected as representative. The other features in the group were removed.

The data were split into a training and test dataset using a stratified fivefold cross-validation. Within the training dataset, feature ranking and selection were performed with lasso regression using a nested fivefold cross-validation. The feature set with the lowest mean squared error (MSE) between the prediction and true label was selected and used for further analysis. To ensure that the minimal MSE was not missed due to the search grid being too large or the step size too small, the grid size was minimized and the step size was tripled.

Next, a logistic regression model using the selected feature set was trained on the full training dataset and, subsequently, tested on the test dataset.

#### Support vector machine model

The data were split into a training and test dataset using a stratified fivefold cross-validation. Within the training dataset, feature ranking and selection were performed using sequential forward feature selection with a nested fivefold cross-validation and included hyperparameter optimization. To this end, the Matlab function *hyperparameters* optimized the box constraint and kernel scale. The feature set with the lowest MSE between the prediction and true label was selected and used for further analysis.

Next, an SVM model using the selected feature set was trained on the full training dataset and included hyperparameter optimization. Subsequently, this model was tested on the test dataset. The adopted kernel type was a radial base function.

#### Assessment of model performance

For both model types, the model performance was assessed in the training and test datasets with sensitivity, specificity, AUROC, positive predictive value (PPV), negative predictive value (NPV), and F1 score. Regarding the sensitivity and

**Table 1** Overview of the carotid ultrasound-based and clinical features that were studied. Per feature, the source necessary for its computation is specified. A description or formula is added if appropriate. If a feature was extracted per beat, the values were averaged to obtain a single value for the measurement period

Source	Feature (units)	Description or formula, if appropriate
Carotid ultrasound – velocity waveform	Peak systolic velocity (PSV) per beat (cm/s)	Maximal amplitude per beat
	Systolic foot velocity (SFV) per beat (cm/s)	Amplitude of the systolic foot per beat
	Mean of the velocity waveform (cm/s)	Mean value of the entire velocity waveform
	Velocity time integral (VTI) per beat (cm)	The area under the velocity waveform for a single beat
	Interdecile range (cm/s)	90 <sup>th</sup> – 10 <sup>th</sup> quantile values of the velocity waveform
	Signal stability index (no unit)	A heuristic measure of the quality of the signal based on the kernel density estimate, as described in (Joshi et al. 2018)
	Signal instability index (no unit)	Bandwidth of the kernels from the kernel density estimate, as described in (Joshi et al. 2018)
	Skewness of the velocity waveform (no unit)	A measure of the asymmetry of the distribution around the sample mean. A positive skewness implies that the data spreads out to the left of the sample mean
	Kurtosis of the velocity waveform (no unit)	A measure that defines how heavily the tails of a distribution differ from the tails of a normal distribution, i.e., whether the tails contain extreme values. A positive kurtosis refers to a heavy-tailed distribution, indicating large outliers
	Pulsatility index (no unit)	$\frac{PSV - SFV}{\text{mean of the velocity waveform}}$
Resistive index (no unit)	$\frac{PSV - SFV}{PSV}$	
Corrected carotid flow time (ccFT) (ms)	$\frac{\text{systolic flow time}}{\sqrt{\text{cycle time}}}$	
Respirophasic peak velocity variation ( $\Delta V_{peak}$ ) (%)	$\frac{PSV_{max} - PSV_{min}}{\frac{1}{2}(PSV_{max} + PSV_{min})} \times 100\%$	
Carotid ultrasound – ensemble average of the velocity waveform	Acceleration (cm/s <sup>2</sup> )	$\frac{PSV - SFV}{\text{rise time}}$
	Relative acceleration time (no unit)	$\frac{\text{rise time}}{\text{length of the cardiac cycle}}$
	Deceleration (cm/s <sup>2</sup> )	$\frac{PSV - SFV}{\text{fall time}}$
	Full-width half-maximum (FWHM) (s)	The width of the waveform shape at half (50%) of its maximum amplitude
	Relative FWHM (no unit)	$\frac{FWHM}{\text{length of the cardiac cycle}}$
	Ratio of the full-width at 75% of the peak to the full-width at 50% of the peak (FWQ3_to_FWHM) (no unit)	$\frac{\text{full-width at 75\% maximum amplitude}}{FWHM}$
	Velocity-based flow augmentation index (FAI) (no unit)	$\frac{\text{secondary systolic peak} - SFV}{PSV - SFV}$
Electronic health record	Age (years)	
	Sex	
	Weight (kg)	
	Height (m)	
	American Society of Anesthesiologists (ASA) class (no unit)	
	Fasting time (min)	
Baseline measurements	Baseline systolic blood pressure (SBP) (mmHg)	Noninvasively obtained with a brachial cuff
	Baseline mean arterial pressure (MAP) (mmHg)	Noninvasively obtained with a brachial cuff

ASA class American Society of Anesthesiologists classification, ccFT corrected carotid flow time,  $\Delta V_{peak}$  respirophasic peak velocity variation, MAP mean arterial pressure, FAI flow augmentation index, FWHM full-width half-maximum, FWQ3\_to\_FWHM ratio of the full-width at 75% of the peak to the FWHM, PSV peak systolic velocity, SBP systolic blood pressure, SFV systolic foot velocity, VTI velocity time integral

**Table 2** Baseline characteristics of the studied population

	All patients, n = 40	Normotensive patients, n = 22 (55%)	Hypotensive patients, n = 18 (45%)	p-value
Sex M/F (%)	65/35	73/27	56/44	0.27
Age, years [IQR]	68 [60–74]	66 [60–71]	73 [64–75]	0.10
Height, cm [IQR]	175 [166–182]	174 [167–183]	176 [165–180]	0.94
Weight, kg [IQR]	78 [71–93]	74 [70–80]	90 [75–103]	< 0.01
BMI, kg/m <sup>2</sup> [IQR]	25.3 [23.7–27.9]	23.8 [22.8–25.6]	27.5 [25.3–30.1]	< 0.01
BSA, m <sup>2</sup> [IQR]	2.0 [1.8–2.2]	1.9 [1.8–2.0]	2.1 [1.9–2.3]	0.02
ASA class I/II/III (%)	20/57/23	32/59/9	6/55/39	< 0.01
Preoperative fasting time, min [IQR]	315 [180–630]	240 [180–420]	405 [210–660]	0.06
Vascular disease, n (%)	4 (10)	2 (9)	2 (11)	0.84
LVF, moderate/good/ unknown (%)	3/22/75	5/27/68	0/17/83	0.22
RVF, moderate/good/ unknown (%)	3/22/75	5/27/68	0/17/83	0.21
Fluids before spinal anesthesia, mL [IQR]	50 [0–100]	25 [0–50]	63 [25–100]	0.48
Fluids after spinal anesthesia, mL [IQR]	125 [100–163]	105 [50–150]	150 [125–200]	0.01

ASA class American Society of Anesthesiologists classification, BMI body mass index, BSA body surface area, F female, IQR interquartile range, LVF left ventricular function, M male, RVF right ventricular function

specificity, the threshold value was determined by maximizing the Youden index in the training dataset. An AUROC value of 0.50–0.59 classifies as no, 0.60–0.69 as poor, 0.70–0.79 as fair, 0.80–0.89 as good, and 0.90–1.0 as excellent discrimination (Nahm 2022). The F1 score is a metric that combines the PPV and sensitivity into a single value, balancing the accuracy of positive predictions with the ability to identify all positive instances (Chinchor 1992). This score is a value between zero and one, with one indicating that the model accurately predicted each label.

We investigated the predictive value of CDU-based and clinical features individually as well as combined.

### Statistical analysis

Statistical analysis was performed using IBM SPSS Statistics version 28.0 (IBM Corporation, IL, USA) and MATLAB version 2023a (Mathworks, MA, USA). Continuous variables were expressed as mean ± standard deviation or median and interquartile range (IQR), depending on normality. Normality was numerically assessed using a Shapiro–Wilk test. The dataset was divided into hypotensive and normotensive patients according to the occurrence of SAIH. Differences in continuous variables between the two groups were studied using the t-test or Mann–Whitney U test, depending on normality. Differences in categorical variables were studied using the chi-squared test. Statistical significance was set at  $p < 0.05$ .

### Results

A total of 44 patients were enrolled in this study. Four were excluded, one due to previously unknown atrial fibrillation, one due to unexpected carotid stenosis of > 50%, and

two due to technical issues. The remaining 40 patients were included in the analysis, of whom 18 patients (45%) developed hypotension. The median age of the patients was 68 [60–74] years and 65% of all patients were men. Table 2 shows the baseline patient characteristics.

### Logistic regression model

Transitive closure led to removing 8 CDU-based features: ‘Peak systolic velocity’, ‘Mean velocity’, ‘Systolic foot velocity’, ‘Interdecile range’, ‘VTI per beat’, ‘Skewness’, ‘Resistance index’, and ‘FWHM’. The remaining 20 features (12 CDU-based and 8 clinical features) were used for further analysis.

Table 3 reports the logistic regression model’s performances on the test dataset when studying the CDU and clinical features individually and combined. While the model using CDU-based features only performed poorly, the model combining CDU-based and clinical features performed best.

Table 4 presents the features that were selected per fold of this best-performing model. The clinical features ‘Baseline MAP’, ‘Fasting time’, ‘ASA class’, and ‘Weight’ were selected in each of the five folds. In contrast, CDU-based features were selected in two folds only. Moreover, the selected CDU features differed per fold, indicating limited predictive value. The feature sets per fold for the logistic regression models using only CDU-based features and only clinical features are reported in Appendix A2.

### Support vector machine model

The SVM model’s performances are shown in Table 5. All SVM models performed poorly, whether using

**Table 3** Performance of the logistic regression models when inputting CDU-based features, clinical features, or a combination of both. Reported values are median [IQR]

	CDU-based features	Clinical features	CDU-based and clinical features
Sensitivity (%)	100 [46 – 100]	67 [25 – 81]	75 [63 – 81]
Specificity (%)	0 [0 – 34]	80 [58 – 100]	75 [71 – 81]
AUROC	0.50 [0.50 – 0.51]	0.81 [0.81 – 0.89]	0.81 [0.75 – 0.95]
PPV (%)	40 [36 – 50]	75 [58 – 100]	75 [65 – 81]
NPV (%)	0 [0 – 40]	67 [57 – 81]	75 [71 – 88]
F1 score	0.55 [0.42 – 0.67]	0.57 [0.40 – 0.71]	0.75 [0.71 – 0.76]

AUROC area under the receiver operating characteristic curve, CDU carotid Doppler ultrasound, NPV negative predictive value, PPV positive predictive value

**Table 4** Selected features per fold of the best-performing logistic regression model, using both CDU-based and clinical features

	Fold 1	Fold 2	Fold 3	Fold 4	Fold 5
FWQ3_to_FWHM					x
Signal stability index					x
Pulsatility index				x	
Signal instability index				x	
Age		x			x
Baseline MAP	x	x	x	x	x
Fasting time	x	x	x	x	x
ASA class	x	x	x	x	x
Weight	x	x	x	x	x

ASA class American Society of Anesthesiologists classification, FWQ3\_to\_FWHM ratio of the full-width at 75% of the peak to the full-width half-maximum, MAP mean arterial pressure

CDU-based features only, clinical features only, or a combination of both. The feature sets per fold are presented in Appendix A3.

When comparing the linear and nonlinear models' performances (Tables 3 and 5), the logistic regression model using features from both feature sources performed best.

### Discussion

This prospective observational study investigated CDU-derived and clinical features for their predictive value of SAIH. All measurements were obtained well in advance of conducting spinal anesthesia. SAIH occurred in 45% of patients. Whether assuming a linear or nonlinear relationship between features and outcome, CDU measurements alone did not demonstrate predictive value for SAIH. The best-performing model combined CDU-based and clinical features in a linear fashion (AUROC 0.81 [0.75–0.95]). The following

**Table 5** Performance of the SVM models when inputting CDU-based features, clinical features, or a combination of both. Reported values are median [IQR]

	CDU-based features	Clinical features	CDU-based and clinical features
Sensitivity (%)	25 [19 – 38]	75 [0 – 100]	0 [0 – 63]
Specificity (%)	75 [58 – 85]	75 [0 – 85]	50 [19 – 63]
AUROC	0.47 [0.39 – 0.62]	0.50 [0.47 – 0.66]	0.38 [0.25 – 0.52]
PPV (%)	33 [25 – 75]	38 [0 – 56]	0 [0 – 38]
NPV (%)	57 [53 – 60]	50 [0 – 62]	33 [25 – 41]
F1 score	0.33 [0.21 – 0.44]	0.55 [0 – 69]	0 [0 – 0.47]

AUROC area under the receiver operating characteristic curve, CDU carotid Doppler ultrasound, NPV negative predictive value, PPV: positive predictive value

features were found to have predictive value: 'Baseline MAP', 'Fasting time', 'ASA class', and 'Weight'.

CDU measurements alone did not demonstrate predictive value for SAIH. The performance of both model types was poor. While we studied simple landmarks and new features obtained from the carotid velocity waveform, known carotid ultrasound parameters, such as the ccFT, were also investigated. The ccFT might predict fluid responsiveness (Barjaktarevic et al. 2018; Suriani et al. 2022), hypotension after general anesthesia (Maitra et al. 2020; Wang et al. 2022), and SAIH in parturient women (Kim et al. 2021). However, consistent with existing literature on non-cardiac surgery patients (Kim et al. 2022), our findings suggest that the ccFT is not a reliable predictor of SAIH in this population.

The best-performing model was found when linearly combining CDU-based and clinical features. These findings suggest that adding hemodynamic characteristics to general clinical measures improves the prediction of SAIH. However, a specific CDU-based feature with predictive value could not be identified, as the selected features differed per fold. Moreover, only in two out of five folds a CDU-based feature was selected. Furthermore, the necessity for additional measurements to obtain CDU-based features is clinically impractical. While the carotid measurements were performed manually in the present study, the recent development of carotid patches would mitigate this issue. A carotid ultrasound patch enables continuous measurements of this central vessel (Kenny et al. 2021; Wang et al. 2022). To our knowledge, this is the first study combining CDU-based and clinical features for the prediction of SAIH.

The predictive value of clinical variables was more apparent. The feature selected in each linear model studying clinical features was 'Weight'. BMI is a known risk factor for SAIH (Carpenter et al. 1992; Hartmann et al. 2002; Singla et al. 2006). We decided to provide weight and height

as individual features instead of combining them into the BMI, as both factors influence the distribution of a local anesthetic differently. Specifically, a high weight and a short height both increase the peak block height, thereby increasing the risk of hypotension. However, the fact that the local anesthetics dosage was determined based on a patient's height in this study can explain why only weight was selected as a predictor. Moreover, in the best-performing logistic regression model, 'Baseline MAP', 'Fasting time', and 'ASA class' were selected in all five folds. Other studies have found baseline SBP or diastolic blood pressure (DBP) to be a risk factor for SAIH (Carpenter et al. 1992; Singla et al. 2006). Lin et al. (Lin et al. 2008) developed an artificial neural network to predict SAIH, achieving an AUROC of 0.80. In line with our findings, their feature set included the features 'Weight', 'ASA class', 'Baseline SBP', and 'Baseline DBP'.

The SVM models did not outperform the logistic regression models, which could suggest that the features follow a linear relationship. However, since a nonlinear model requires a larger dataset than a linear model, the relatively small dataset of our study could also explain the lower performance of the SVM models.

The type and settings of the feature selector play an important role in the selection of features. We used lasso regression for the logistic regression models, which selected the feature sets based on the lowest MSE between the prediction and the label. Another criterion often used is selecting the feature set with the lowest MSE + 1 standard deviation. However, as this results in fewer features being selected, this criterion was deemed too strict for our study. For the nonlinear SVM model, sequential forward feature selection was used instead of lasso, as the latter assumes a linear relationship between features and labels. We tried to improve the stability of the feature selection process by using nested fivefold cross-validation. However, as seen from Table 5 and Appendix A3 the results of the SVM models were rather unstable. This is mostly caused by the SVM models' higher variance in combination with the small dataset.

In this study, the time window between the measurement period and the induction of spinal anesthesia was at least 10 min. In contrast, the predictive model of Lin et al. used measurements obtained close to the induction of spinal anesthesia (Lin et al. 2008). Being able to predict SAIH minutes before its onset would give anesthesiologists ample time to intervene.

Another factor influencing the incidence of hypotension is the timing of the baseline blood pressure measurement. In this study, the blood pressure was measured twice before the spinal anesthesia procedure: once before the patient entered the operating room ( $T_{\text{baseline}}$ ) and once in the operating room immediately before the induction of spinal anesthesia ( $T_0$ ). It was noticed that patients were generally more nervous at  $T_0$ , resulting in

elevated blood pressure values. It was reasoned that using  $T_0$  to compute the percentage decrease in blood pressure would overestimate the incidence of SAIH. Therefore,  $T_{\text{baseline}}$  was used for this calculation.

The full potential of the features that can be extracted from carotid ultrasound images remains partly unexplored. This study specifically focused on velocity-based features. However, B-mode images can also be obtained using carotid ultrasound, allowing for the extraction of diameter waveforms and, subsequently, diameter-based features. A more in-depth investigation into these features may provide valuable insights.

This study has several limitations. The first one encompasses the utilized dataset (post-hoc analysis of previously acquired data) and is simultaneously a strength of this study. Analyzing real-world clinical data gives a correct image of clinical practice and its patients, but the used dataset consisted of data from a small number of patients. In general, a small dataset makes it challenging to describe nonlinearities and limits the number of features that can be studied. To optimally use the available data, a fivefold cross-validation was employed. Moreover, with the goal of feature dimensionality reduction, cross-correlation with transitive closure, and feature ranking and selection were performed. We believe that the usage of clinical data in this study can guide future studies with large clinical populations. As an alternative to the time-consuming process of obtaining a large clinical dataset, future studies could involve the analysis of so-called virtual populations, i.e., simulated data (Suriani et al. 2024).

Second, the lack of a standard definition for SAIH might have influenced our results. Blijker et al. (Bijker et al. 2007) showed that the incidence of hypotension after general anesthesia varies between 5 and 99%, depending on the definition used. We used the definition utilized in the dataset's original study (van Houte et al. 2024), which is believed to be reasonably chosen (Bijker et al. 2007). It resulted in an incidence of SAIH of 45%, which is in line with previously reported values ranging from 18 to 50% (Chowdhury et al. 2023; Jakobsson et al. 2017).

Third, although an expert sonographer obtained the CDU images, it should be noted that performing these measurements was still a manual process that is prone to measurement error. A carotid patch, integrated with automated software, will likely improve measurement accuracy and precision.

## Conclusion

In conclusion, preoperative SAIH prediction was better achieved by linearly combining CDU-based and clinical features, rather than relying on CDU-based features alone. The clinical variables baseline MAP, fasting time, ASA class, and weight were shown to have predictive value for SAIH.

**Abbreviations**

ASA class	American Society of Anesthesiologists classification
AUROC	Area under the receiver operating characteristic curve
BMI	Body mass index
ccFT	Corrected carotid flow time
CDU	Carotid Doppler ultrasound
DBP	Diastolic blood pressure
ECCG	Electrocardiogram
FWHM	Full-width half-maximum
FWQ3	Full-width at 75% of the maximal amplitude
FWQ3_to_FWHM	Ratio of the FWQ3 and FWHM
IQR	Interquartile range
MAP	Mean arterial pressure
MSE	Mean squared error
NIBP	Noninvasive blood pressure
PWD	Pulsed-wave Doppler
SAIH	Spinal anesthesia-induced hypotension
SBP	Systolic blood pressure
SVM	Support vector machine
VTI	Velocity time integral

**Supplementary Information**

The online version contains supplementary material available at <https://doi.org/10.1186/s13741-025-00508-w>.

Supplementary Material 1. Appendix

**Acknowledgements**

The study was performed within Eindhoven MedTech Innovation Center (e/MTIC), a research collaboration of academic, clinical, and industrial partners in Eindhoven.

**Authors' contribution**

EdB worked on the study conception, designed the work, performed the data analysis, interpreted the data, created software to analyze the data, and drafted the manuscript. JvH worked on the study conception, designed the work, performed the data acquisition, and interpreted the data. CDF worked on the study conception and data interpretation, and she revised the manuscript. TB interpreted the data and revised the manuscript. JM revised the manuscript. AB worked on the study conception and revised the manuscript. MM worked on the study conception and revised the manuscript. All authors read and approved the final manuscript.

**Funding**

The project in which this research was conducted (BRUM project, number 17878) is funded by the Dutch Research Council (NWO). Nederlandse Organisatie voor Wetenschappelijk Onderzoek, 17878

**Data availability**

The data used and/or analyzed during the current study are available from the corresponding author upon reasonable request.

**Declarations****Ethics approval and consent to participate**

All patients who participated in this study gave their written informed consent. Previously acquired data (van Houte et al. 2024) was used to perform the analysis, which was approved by the Medical Research Ethics Committees United (W22.234).

**Consent for publication**

Not applicable.

**Competing interests**

AB acts as a clinical consultant for Philips Research in Eindhoven, The Netherlands, and receives consultant honoraria for this work. The remaining authors declare that they have no competing interests.

**Author details**

<sup>1</sup>Department of Electrical Engineering, Eindhoven University of Technology, Eindhoven, The Netherlands. <sup>2</sup>Department of Anesthesiology, Catharina Hospital, Eindhoven, The Netherlands. <sup>3</sup>Hospital Patient Monitoring, Philips Research, Eindhoven, The Netherlands.

Received: 6 December 2024 Accepted: 23 February 2025

Published online: 08 March 2025

**References**

- Barjaktarevic I, Toppen WE, Hu S, Montoya EA, Ong S, Buhr R, et al. Ultrasound Assessment of the Change in Carotid Corrected Flow Time in Fluid Responsiveness in Undifferentiated Shock. *Crit Care Med*. 2018;46(11):1040–6 Lippincott Williams and Wilkins.
- Bijker JB, Van Klei WA, Kappen TH, Van Wolfswinkel L, Moons KGM, Kalkman CJ. Incidence of Intraoperative Hypotension as a Function of the Chosen Definition Literature Definitions Applied to a Retrospective Cohort Using Automated Data Collection. *Anesthesiol*. 2007;2(107):213–20.
- Carpenter R, Caplan R, Brown D, Stephenson C, Wu R. Incidence and Risk Factors for Side Effects of Spinal Anesthesia. *Anesthesiol*. 1992;76(6):906–16.
- Chinchor N. MUC-4 evaluation metrics. Fourth Message Understanding Conference (MUC-4): Proceedings of a Conference Held in McLean, Virginia, June 16–18, 1992. 1992. p. 22–9.
- Chowdhury SR, Datta PK, Maitra S, Rawat D, Baidya DK, Roy A, et al. The use of preoperative inferior vena cava ultrasound to predict anaesthesia-induced hypotension: a systematic review. *Anaesthesiol Intensive Ther*. 2023;55(1):18–31 Termedia Publishing House Ltd.
- Hartmann B, Junger A, Klasen J, Benson M, Jost A, Banzhaf A, et al. The Incidence and Risk Factors for Hypotension After Spinal Anesthesia Induction: An Analysis with Automated Data Collection. *Anesth Analg*. 2002;94:1521–9.
- Henzinger MR, King V. Fully dynamic biconnectivity and transitive closure. Proceedings of IEEE 36th Annual Foundations of Computer Science. Milwaukee, WI, USA: IEEE Comput. Soc. Press; 1995. p. 664–72.
- van Houte J, de Boer EC, Manning F, van Suijlekom FSLC, Van 't Veer M, Bouwman AR. The corrected carotid artery flow time and carotid peak velocity variation do not predict spinal anesthesia-induced hypotension: A prospective observational study. *JCA Advances*. 2024;1:1–8. Elsevier BV.
- Jakobsson J, Kalman SH, Lindeberg-Lindvet M, Bartha E. Is postspinal hypotension a sign of impaired cardiac performance in the elderly? An observational mechanistic study. *Br J Anaesth*. 2017;119(6):1178–85 Oxford University Press.
- Joshi R, Bierling BL, Long X, Weijers J, Feijs L, Van Pul C, et al. A ballistographic approach for continuous and non-obtrusive monitoring of movement in neonates. *IEEE J Transl Eng Health Med*. Institute of Electrical and Electronics Engineers Inc.; 2018;6.
- Kenny JÉS, Munding CE, Eibl JK, Eibl AM, Long BF, Boyes A, et al. A novel, hands-free ultrasound patch for continuous monitoring of quantitative Doppler in the carotid artery. *Sci Rep*. 2021;11(1):1–11 Nature Research.
- Kim HJ, Choi YS, Kim SH, Lee W, Kwon JY, Kim DH. Predictability of preoperative carotid artery-corrected flow time for hypotension after spinal anaesthesia in patients undergoing caesarean section: A prospective observational study. *Eur J Anaesthesiol*. 2021;38(4):394–401 Lippincott Williams and Wilkins.
- Kim HJ, Cho AR, Lee H, Kim H, Kwon JY, Lee HJ, et al. Ultrasonographic Carotid Artery Flow Measurements as Predictors of Spinal Anesthesia-Induced Hypotension in Elderly Patients: A Prospective Observational Study. *Medical Science Monitor*. 2022;28:1–10. International Scientific Information, In.
- Lin CS, Chiu JS, Hsieh MH, Mok MS, Li YC, Chiu HW. Predicting hypotensive episodes during spinal anesthesia with the application of artificial neural networks. *Comput Methods Programs Biomed*. 2008;92(2):193–7.
- Maitra S, Baidya DK, Anand RK, Subramaniam R, Bhattacharjee S. Carotid Artery Corrected Flow Time and Respiratory Variations of Peak Blood Flow Velocity for Prediction of Hypotension After Induction of General Anesthesia in Adult Patients Undergoing Elective Surgery: A Prospective Observational Study. *J Ultrasound Med*. 2020;39(4):721–30 John Wiley and Sons Ltd.
- Mendonça FT, Crepaldi Junior LC, Gersanti RC, de Araujo KC. Effect of ondansetron on spinal anesthesia-induced hypotension in non-obstetric surgeries: a randomised, double-blind and placebo-controlled trial. *Braz J Anesthesiol*. 2021;71(3):233–40. Elsevier Editora Ltda.

- Meyhoff CS, Haarmark C, Kanters JK, Rasmussen LS. Is it possible to predict hypotension during onset of spinal anesthesia in elderly patients? *J Clin Anesth.* 2009;21(1):23–9.
- Nahm FS. Receiver operating characteristic curve: overview and practical use for clinicians. *Korean J Anesthesiol.* 2022;75(1):25–36 Korean Society of Anesthesiologists.
- Rivers E, Nguyen B, Havstad S, Ressler J, Muzzin A, Knoblich B, et al. Early Goal-Directed Therapy in the Treatment of Severe Sepsis and Septic Shock. *N Engl J Med.* 2001;345(19):1368–77.
- Sessler DI, Bloomstone JA, Aronson S, Berry C, Gan TJ, Kellum JA, et al. Perioperative Quality Initiative consensus statement on intraoperative blood pressure, risk and outcomes for elective surgery. *Br J Anaesth.* 2019;122(6):719–22 Elsevier Ltd.
- Singla D, Kathuria S, Singh A, Kaul TK, Gupta S. Risk Factors for Development of Early Hypotension during Spinal Anaesthesia. *J Anaesthesiol Clin Pharmacol.* 2006;22(4):387–93.
- Suriani I, van Houte J, de Boer EC, van Knippenberg L, Manzari S, Mischi M, et al. Carotid Doppler ultrasound for non-invasive haemodynamic monitoring: a narrative review. *Physiol Meas.* Institute of Physics; 2022;43(10).
- Suriani I, Bouwman RA, Mischi M, Lau KD. An in silico study of the effects of cardiovascular aging on carotid flow waveforms and indexes in a virtual population. *Am J Physiol Heart Circ Physiol.* 2024;326(4):877–99 American Physiological Society.
- Tarkkila P, Isola J. A regression model for identifying patients at high risk of hypotension, bradycardia and nausea during spinal anesthesia. *Acta Anaesthesiol Scand.* 1992;36(6):554–8.
- Walsch M, Devereaux PJ, Garg AX, Kurz A, Turan A, Rodseth RN, et al. Relationship between Intraoperative Mean Arterial Pressure and Clinical Outcomes after Noncardiac Surgery, Toward an Empirical Definition of Hypotension. *Anesthesiol.* 2013;119(3):507–15.
- Wang J, Li Y, Su H, Zhao J, Tu F. Carotid artery corrected flow time and respiratory variations of peak blood flow velocity for prediction of hypotension after induction of general anesthesia in elderly patients. *BMC Geriatr.* 2022;22(1). BioMed Central Ltd.
- Wesselink EM, Kappen TH, Torn HM, Slooter AJC, van Klei WA. Intraoperative hypotension and the risk of postoperative adverse outcomes: a systematic review. *Br J Anaesth.* 2018;706–21. Elsevier Ltd.

## Publisher's Note

Springer Nature remains neutral with regard to jurisdictional claims in published maps and institutional affiliations.